

Reaction cross sections for ${}^8\text{B}$, ${}^7\text{Be}$, and ${}^6\text{Li} + {}^{58}\text{Ni}$ near the Coulomb barrier: Proton-halo effects

E. F. Aguilera,^{1,*} E. Martinez-Quiroz,¹ D. Lizcano,¹ A. Gómez-Camacho,¹ J. J. Kolata,² L. O. Lamm,² V. Guimarães,³ R. Lichtenhaler,³ O. Camargo,³ F. D. Becchetti,⁴ H. Jiang,⁴ P. A. DeYoung,⁵ P. J. Mears,⁵ and T. L. Belyaeva⁶

¹*Departamento de Aceleradores, Instituto Nacional de Investigaciones Nucleares, Apartado postal 18-1027*

C. P. 11801, Mexico, D. F., Mexico

²*Physics Department, University of Notre Dame, Notre Dame, Indiana 46556-5670, USA*

³*Instituto de Fısica, Universidade de Sao Paulo, P. O. Box 66318, 05389-970 Sao Paulo, SP, Brazil*

⁴*Physics Department, University of Michigan, Ann Arbor, Michigan 48109-1120, USA*

⁵*Physics Department, Hope College, Holland, Michigan 49422-9000, USA*

⁶*Universidad Autonoma del Estado de Mexico, Toluca, Mexico*

(Received 27 October 2008; published 5 February 2009)

Elastic scattering of ${}^8\text{B}$, ${}^7\text{Be}$, and ${}^6\text{Li}$ on a ${}^{58}\text{Ni}$ target has been measured at energies near the Coulomb barrier. Optical-model fits were made to the experimental angular distributions, and total reaction cross sections were deduced. A comparison with other systems provides striking evidence for proton-halo effects on ${}^8\text{B}$ reactions. As opposed to the situation for the neutron-halo nucleus ${}^6\text{He}$, for which particle transfer dominates, the “extra” cross section observed for ${}^8\text{B}$ appears to result entirely from projectile breakup.

DOI: [10.1103/PhysRevC.79.021601](https://doi.org/10.1103/PhysRevC.79.021601)

PACS number(s): 25.60.Bx, 25.60.Dz, 25.70.−z

The short-lived radioactive nucleus ${}^8\text{B}$ is adjacent to the proton drip line and has a very small proton separation energy of only 0.138 MeV. In addition to its role in the production of high-energy neutrinos in the Sun [1–5], it has attracted much attention in the last decade because it may have a proton halo [6–8]. Some breakup (*bu*), quasi-elastic, and total reaction cross section measurements at energies much above the Coulomb barrier [9–15] have indicated an extended spatial distribution for the loosely bound proton in ${}^8\text{B}$, but the question of the existence of a proton halo has remained open [16,17]. More recently [18,19], an angular distribution for the *bu* of ${}^8\text{B}$ on a ${}^{58}\text{Ni}$ target measured at a near-barrier energy indicated that Coulomb-nuclear interference at very large distances plays an important role. This reinforces the idea of the exotic proton-halo nature of this nucleus. Calculations treating the projectile as a weakly bound proton orbiting a ${}^7\text{Be}$ core reproduce the data quite well as long as continuum-continuum couplings are included [18,20–22]. Single-angle measurements at 25, 26.9, and 28.4 MeV gave consistent values for the absolute cross sections in agreement with the predicted trend [23]. Additional evidence for the proton halo of ${}^8\text{B}$, both theoretical and experimental, has appeared in the literature in recent years [24–31].

One might wonder whether the near- and sub-barrier reaction yields for this system would show similarities with, e.g., previous observations for the neutron-halo projectile ${}^6\text{He}$, where large enhancements are observed below the barrier with a ${}^{209}\text{Bi}$ target [32–34], and also for targets closer to ${}^{58}\text{Ni}$ [35,36]. (For systems with lighter targets such as ${}^6\text{He} + {}^{12}\text{C}$ [37] and ${}^6\text{He} + {}^{27}\text{Al}$ [38] the neutron halo effects seem to be smaller.) While much work has been done on neutron-halo nuclei [39,40] the present knowledge of proton-halo effects is rather scarce [41]. Rehm *et al.* [42] have studied the fusion of ${}^{17}\text{F} + {}^{208}\text{Pb}$ and found a slightly reduced fusion cross section

below the barrier. Liang *et al.* [43] have measured *bu* of ${}^{17}\text{F}$ on ${}^{208}\text{Pb}$ and found a very small cross section. It is not clear, however, that either of these experiments gives relevant information on the effect of the proton-halo state, which is an excited state in ${}^{17}\text{F}$. The probability of Coulomb Excitation to the halo state during the fusion reaction is very small [42], so the proton halo likely did not come into play. Also, the *bu* experiment was performed at an energy well above the Coulomb barrier and in an angular range where absorption via the imaginary part of the optical potential is very large, so peripheral breakup, which is sensitive to the halo state, was not being probed. Similar considerations apply also to recent measurements for proton-rich isotopes of phosphorus [44]. As a result, it is far from clear that enhanced cross sections should be expected in the proton-halo case and it is therefore important that reaction yields near the barrier be studied for true proton-halo systems. Along these lines, elastic scattering measurements are reported here for ${}^8\text{B}$ and also its core, the radioactive nucleus ${}^7\text{Be}$. For further comparison, additional data for the stable but weakly-bound projectile ${}^6\text{Li}$ were also obtained. Preliminary results for ${}^8\text{B}$ have been reported earlier in the form of Conference Proceedings [45].

A ${}^8\text{B}$, ${}^7\text{Be}$, ${}^6\text{Li}$ “cocktail” beam was produced by the TwinSol radioactive nuclear beam facility at the University of Notre Dame [46]. A primary beam of ${}^6\text{Li}$ at energies of 29, 31, 33, 35, and 37 MeV was incident on a ${}^3\text{He}$ gas-cell production target. The corresponding laboratory energies of the secondary beams, at the target center, were 20.7, 23.4, 25.3, 27.2, and 29.3 MeV for ${}^8\text{B}$; 15.1, 17.1, 18.5, 19.9, and 21.4 MeV for ${}^7\text{Be}$; and 9.9, 11.2, 12.1, 13.0, and 14.0 MeV for ${}^6\text{Li}$. The typical primary beam current was 250 particle nA, giving typical secondary beam rates for ${}^8\text{B}$, ${}^7\text{Be}$, and ${}^6\text{Li}$ of 4.0×10^4 , 7.3×10^4 , and 6.0×10^5 particles/s, respectively. The corresponding energy widths (FWHM) were 0.86, 1.11, and 0.90 MeV. An enriched ${}^{58}\text{Ni}$ target with a thickness of 0.924 mg/cm² was used for all energies except the lowest one, where the thickness was 0.98 mg/cm².

*eli.aguilera@inin.gob.mx

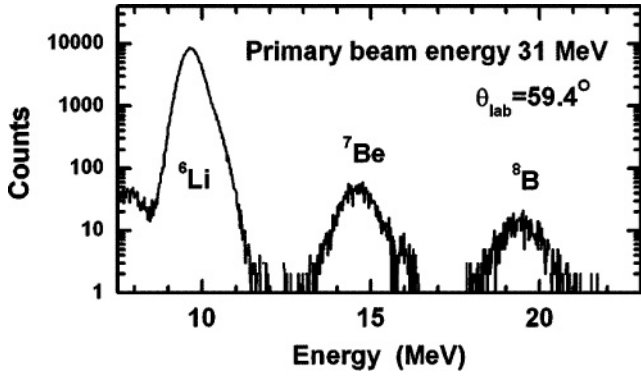


FIG. 1. One-dimensional spectrum obtained with a PSD. The elastic scattering peaks for ^8B , ^7Be , and ^6Li are indicated.

The scattered particles were detected with four 24×24 mm Si position-sensitive detectors (PSDs) and one $E-\Delta E$ silicon-detector telescope. The detectors were moved to cover both forward and backward angles. When used at small forward angles, where good statistics are obtained, the PSDs were software sectioned into two halves in order to obtain data at additional angles. A typical spectrum obtained with a PSD is presented in Fig. 1. The three elastic peaks are clearly separated in this spectrum, and the data from the telescope confirmed that contamination from other ions was negligible. The energy resolution was sufficient to separate the ^{58}Ni first excited state (2^+ , 1.45 MeV), which we did not see for any projectile. For ^8B and ^6Li , which have no bound excited states, the data are then purely elastic. On the other hand, ^7Be has a low-lying bound state at 0.43 MeV that cannot be resolved, so any corresponding inelastic yield is included in the data.

The experimental angular distributions for (^8B , ^7Be , ^6Li) + ^{58}Ni are shown in Fig. 2. For the first system, the best optical-model description of the data was obtained with real and imaginary potentials of the Woods-Saxon type suitably adjusted for each bombarding energy. The corresponding potential parameters are indicated in Table I and the calculations are represented by the curves shown in Fig. 2. All χ^2/N values reported in this work refer to χ^2 per point. Other potentials having different, deeper real-well depths gave equivalent fits. These ambiguities, however, are not relevant for the present work since the total reaction cross section values calculated with all well geometries were equivalent as long as the experimental angular distribution was properly fitted. It is worth

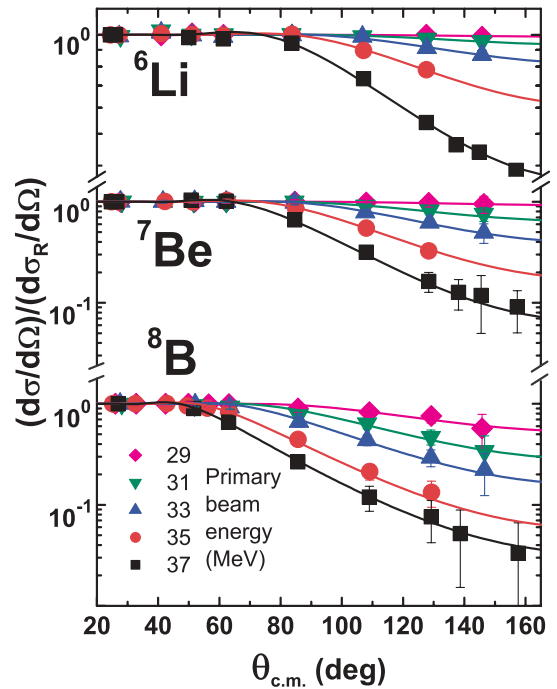


FIG. 2. (Color online) Elastic scattering angular distributions for (^8B , ^7Be , ^6Li) + ^{58}Ni at the five energies indicated. If not shown, error bars (purely statistical) are smaller than the size of the symbol. The curves correspond to optical model calculations with the potentials of Tables I and II.

pointing out that every acceptable potential had an imaginary part that extended beyond the corresponding real part. This suggests absorption at a large distance due to the existence of a halo state. The reaction cross sections are given in Table I.

In the case of the ^7Be projectile, the inelastic scattering contribution to the quasi-elastic scattering was ignored in the optical model analysis. Reported measurements [47] for the mirror nucleus ^7Li , which has a similar low-energy excited state, show that the corresponding inelastic contribution is negligibly small. For the (^7Be , ^6Li) + ^{58}Ni systems, the Sao Paulo potential (SPP) [48] was used for the real part while the imaginary part was obtained by multiplying the real part times a factor N_I . This factor was chosen to fit the data for each energy, with the results shown in Table II. A good description of the data was obtained, as shown by the corresponding curves in Fig. 2. For ^6Li + ^{58}Ni , data previously taken [49]

TABLE I. Optical-model potentials obtained for ^8B + ^{58}Ni and the corresponding calculated reaction cross sections. The real and imaginary parts are volume Woods-Saxon type with radii given by $R_x = r_x \times (A_p^{1/3} + A_T^{1/3})$. The depth is in MeV and the radius and diffuseness are in fm. The Coulomb radius is $r_C = 1.2$ fm.

E_{lab}	V	r_R	a_R	W_V	r_I	a_I	χ^2/N	$\sigma_R(\text{mb})$
20.7	10.0	1.30	0.56	166.9	1.26	0.65	0.15	198 ± 50
23.4	11.8	1.30	0.53	166.8	1.22	0.61	0.58	363 ± 50
25.3	11.9	1.28	0.54	166.8	1.21	0.60	0.33	512 ± 50
27.2	10.8	1.30	0.53	166.9	1.24	0.62	0.41	812 ± 45
29.3	10.0	1.30	0.52	173.8	1.26	0.61	0.13	1005 ± 40

TABLE II. Optical-model potentials obtained for (${}^7\text{Be}$, ${}^6\text{Li}$) + ${}^{58}\text{Ni}$, and the corresponding calculated reaction cross sections. The SPP is used for the real part V while the imaginary part $W = N_I \times V$.

${}^7\text{Be} + {}^{58}\text{Ni}$				${}^6\text{Li} + {}^{58}\text{Ni}$			
E_{lab}	N_I	χ^2/N	$\sigma_R(\text{mb})$	E_{lab}	N_I	χ^2/N	$\sigma_R(\text{mb})$
15.1	1.7	0.12	20.4 ± 10	9.9	2.0	0.07	4 ± 2.7
17.1	1.5	0.35	106 ± 30	11.2	0.95	0.62	16.3 ± 9
18.5	0.9	0.70	182 ± 26	12.1	0.78	0.11	43.3 ± 12
19.9	0.9	0.68	330 ± 101	13.0	0.78	0.04	108 ± 36
21.4	1.0	1.12	506 ± 97	14.0	0.95	1.37	235 ± 52

and recently reanalyzed [50] give total reaction cross sections consistent with our values.

The total reaction cross sections obtained for ${}^8\text{B} + {}^{58}\text{Ni}$, displayed in Fig. 3 with filled circles, show a very large enhancement with respect to SPP predictions using $N_I = 0.78$ (open circles). The latter represent the values typically expected for “normal” nuclei [51]. A normalization factor $N_I = 3.6$ would be required to fit these data. A fusion excitation function predicted in a one-dimensional barrier penetration model (BPM) is shown for comparison purposes. The corresponding barrier parameters ($V_b = 20.8$ MeV, $\hbar\omega = 4.4$ MeV, $R_b = 8.9$ fm) were obtained from the real SPP plus the Coulomb potential. They are in good agreement with those obtained from well-known empirical formulas [52,53].

An integrated breakup cross section was determined from the data of Ref. [18] and is shown by the square in Fig. 3. A CDCC calculation was performed for ${}^8\text{B}$ breakup as described in Refs. [21–23], including the whole energy region where the present experiment was carried out. It was checked that the results were not sensitive to the optical-model potentials used. This calculation reproduces the measured breakup yield at $E_{\text{lab}} = 25.8$ MeV quite well. (Figure 3 shows the predicted breakup cross section as a function of energy.)

In order to compare the above with existing results for other systems [34,35,54,55], a suitable scaling of the data was made

by dividing the cross sections by the factor $(A_p^{1/3} + A_t^{1/3})^2$ and the energy by the factor $Z_p Z_t / (A_p^{1/3} + A_t^{1/3})$. Arguments have been given demonstrating that this procedure properly scales the normal geometrical and/or charge differences between systems without washing out the dynamical effects of interest [56]. The results, presented in Fig. 4, are quite interesting: the halo systems (${}^6\text{He} + {}^{209}\text{Bi}$, ${}^6\text{He} + {}^{64}\text{Zn}$, ${}^8\text{B} + {}^{58}\text{Ni}$) have very similar reduced cross sections which lie above those for the weakly-bound “normal” nuclei (Li and Be projectiles). The most striking result is that the ${}^8\text{B}$ data show an enhancement similar to that present for the neutron-halo nucleus ${}^6\text{He}$. In semiclassical terms, Coulomb polarization favors neutrons in the halo residing in the region between the core and the target, which then enhances the reaction probabilities. Since these neutrons are closer to the target one can understand that they might tend to be transferred to it, consistent with observations for ${}^6\text{He} + {}^{209}\text{Bi}$. In that system, most of the reaction yield comes from two-neutron transfer to neutron-unbound levels in the reaction product [57]. In contrast, an enhancement driven by particle transfer is not expected for a proton-halo system. Here, one would expect that Coulomb polarization would result in the valence proton spending more time at large distances from the target, shielded by the core from the full Coulomb effect. Core-halo breakup would occur mainly through the long range Coulomb force, and proton transfer

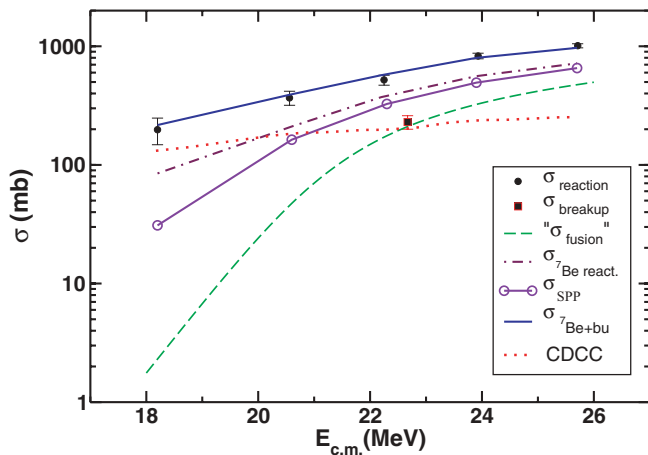


FIG. 3. (Color online) Total reaction and breakup cross sections for ${}^8\text{B} + {}^{58}\text{Ni}$. The various curves represent calculations that are discussed in the text.

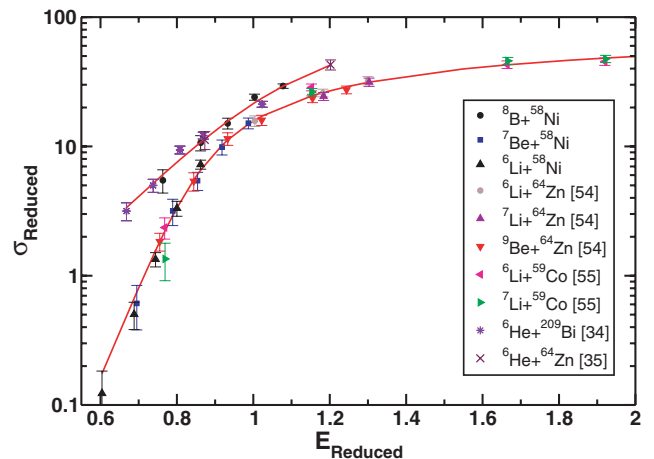


FIG. 4. (Color online) Reduced cross sections from the present work compared with other data. The curves are to guide the eye.

would be suppressed. Esbensen and Bertsch [58] have shown that Coulomb breakup is in fact strongly modified by both the halo nature and the Coulomb polarization of the ^8B projectile. Despite this, the predicted breakup cross section is quite large and in agreement with experiment.

The present work can give some insight into the role of transfer processes in the reactions of proton-halo systems. In this regard, it is interesting to compute the $^8\text{B} + ^{58}\text{Ni}$ total reaction cross section from the ^7Be reduced reaction yield scaled according to the ^8B mass and charge. This is shown by the dot-dashed curve in Fig. 3. While much bigger than the fusion cross section computed from the BPM, it is similar to the total reaction cross section for “normal” nuclei computed from the SPP as discussed above (at least at energies above the Coulomb barrier, i.e., above ~ 21 MeV). However the most important observation is that the sum of this curve plus the ^8B breakup yield from the CDCC calculation reproduces the observed total reaction cross section almost perfectly (Fig. 3). In other words, the ^8B reaction cross section can be entirely accounted for by breakup of the halo state plus reactions that occur with the ^7Be core, leaving no room for proton transfer. This suggests an underlying decoupling between the core and the valence proton, which is an expected feature of a proton-halo state [16]. The present observations can then be taken as providing important evidence in favor of a proton-halo hypothesis for ^8B .

In summary, elastic-scattering angular distributions and total reaction cross sections for the (^8B , ^7Be , ^6Li) + ^{58}Ni systems are reported for energies near the Coulomb barrier. The ^7Be and ^6Li reduced cross sections closely follow the behavior observed for other systems involving weakly-bound projectiles, but are strikingly different from those of ^8B . Comparison of the latter with both the expected values for normal nuclei and data from other systems shows a remarkable enhancement, similar to that present for the neutron-halo projectile ^6He . However, an important qualitative difference between the two cases is noted. The enhancement originates from transfer processes for neutron-halo nuclei, but is apparently due to breakup in the case of the proton halo. The difference can be intuitively understood in semiclassical terms as due to the effect of Coulomb polarization on the halo state. This interesting observation follows from the fact that the difference between the total reaction cross sections for ^8B and its core, ^7Be , after geometry and charge effects are removed, is entirely accounted for by the breakup yield of ^8B .

This work has been partially supported by CONACYT, by FAPESP 2001/06676, and by the US NSF under Grant Nos. PHY06-52591 and PHY07-58100. E.F.A. acknowledges the hospitality of all personnel at the Notre Dame Nuclear Structure Laboratory.

-
- [1] J. N. Bahcall, *Neutrino Astrophysics* (Cambridge University Press, Cambridge, England, 1989).
- [2] C. A. Bertulani, *Phys. Rev. C* **49**, 2688 (1994).
- [3] J. von Schwarzenberg, J. J. Kolata, D. Peterson, P. Santi, M. Belbot, and J. D. Hinnefeld, *Phys. Rev. C* **53**, R2598 (1996).
- [4] H. Esbensen, G. F. Bertsch, and K. A. Snover, *Phys. Rev. Lett.* **94**, 042502 (2005).
- [5] F. Schümann *et al.*, *Phys. Rev. C* **73**, 015806 (2006).
- [6] T. Minamisono *et al.*, *Phys. Rev. Lett.* **69**, 2058 (1992).
- [7] H. Kitagawa and H. Sagawa, *Phys. Lett.* **B299**, 1 (1993).
- [8] H. Nakada and T. Otsuka, *Phys. Rev. C* **49**, 886 (1994).
- [9] W. Schwab *et al.*, *Z. Phys. A* **350**, 283 (1995).
- [10] R. E. Warner *et al.*, *Phys. Rev. C* **52**, R1166 (1995).
- [11] I. Pecina *et al.*, *Phys. Rev. C* **52**, 191 (1995).
- [12] F. Negoita *et al.*, *Phys. Rev. C* **54**, 1787 (1996).
- [13] J. H. Kelley *et al.*, *Phys. Rev. Lett.* **77**, 5020 (1996).
- [14] Y. Penionszhkevich, *Nucl. Phys.* **A616**, 247c (1997).
- [15] M. H. Smedberg *et al.*, *Phys. Lett.* **B452**, 1 (1999).
- [16] S. Mizutori, J. Dobaczewski, G. A. Lalazissis, W. Nazarewicz, and P. G. Reinhard, *Phys. Rev. C* **61**, 044326 (2000).
- [17] Y. Suzuki, R. G. Lovas, K. Yabana, and K. Varga, *Structure and Reactions of Light Exotic Nuclei* (Taylor & Francis, London, 2003).
- [18] V. Guimarães *et al.*, *Phys. Rev. Lett.* **84**, 1862 (2000).
- [19] J. J. Kolata *et al.*, *Phys. Rev. C* **63**, 024616 (2001).
- [20] H. Esbensen and G. F. Bertsch, *Phys. Rev. C* **59**, 3240 (1999).
- [21] F. M. Nunes and I. J. Thompson, *Phys. Rev. C* **59**, 2652 (1999).
- [22] J. A. Tostevin, F. M. Nunes, and I. J. Thompson, *Phys. Rev. C* **63**, 024617 (2001).
- [23] E. F. Aguilera, E. Martínez-Quiroz, T. L. Belyaeva, J. J. Kolata, and R. Leyte-Gonzalez, *Phys. At. Nucl.* **71**, 1163 (2008).
- [24] L. Trache, F. Carstoiu, C. A. Gagliardi, and R. E. Tribble, *Phys. Rev. Lett.* **87**, 271102 (2001).
- [25] D. Cortina-Gil *et al.*, *Phys. Lett.* **B529**, 36 (2002).
- [26] D. Cortina-Gil *et al.*, *Nucl. Phys.* **A720**, 3 (2003).
- [27] R. N. Majumdar, *J. Phys. Soc. Jpn.* **72**, 3087 (2003).
- [28] M. S. Hussein *et al.*, *Phys. Lett.* **B640**, 91 (2006).
- [29] T. Sumikama *et al.*, *Phys. Rev. C* **74**, 024327 (2006).
- [30] C. A. Bertulani, *J. Phys. G: Nucl. Part. Phys.* **34**, 315 (2007).
- [31] S. Karataglidis and K. Amos, *Phys. Lett.* **B650**, 148 (2007).
- [32] J. J. Kolata *et al.*, *Phys. Rev. Lett.* **81**, 4580 (1998).
- [33] E. F. Aguilera *et al.*, *Phys. Rev. Lett.* **84**, 5058 (2000).
- [34] E. F. Aguilera *et al.*, *Phys. Rev. C* **63**, 061603(R) (2001).
- [35] A. DiPietro *et al.*, *Phys. Rev. C* **69**, 044613 (2004).
- [36] A. Navin *et al.*, *Phys. Rev. C* **70**, 044601 (2004).
- [37] M. Milin *et al.*, *Nucl. Phys.* **A730**, 285 (2004).
- [38] E. Benjamim *et al.*, *Phys. Lett.* **B647**, 30 (2007).
- [39] L. F. Canto, P. R. S. Gomes, R. Donangelo, and M. S. Hussein, *Phys. Rep.* **424**, 1 (2006).
- [40] N. Keeley, R. Raabe, N. Alamanos, and J. L. Sida, *Prog. Part. Nucl. Phys.* **59**, 579 (2007).
- [41] Y.-J. Liang *et al.*, arXiv:0708.0071 (2007) (<http://adsabs.harvard.edu/abs/2007arXiv0708.0071>).
- [42] K. E. Rehm *et al.*, *Phys. Rev. Lett.* **81**, 3341 (1998).
- [43] J. F. Liang *et al.*, *Phys. Lett.* **B491**, 23 (2000).
- [44] A. Navin *et al.*, *Phys. Rev. Lett.* **81**, 5089 (1998).
- [45] E. F. Aguilera *et al.*, *Rev. Mex. Fis. S* **54**, 1 (2008).
- [46] M. Y. Lee *et al.*, *Nucl. Instrum. Methods A* **422**, 536 (1999).
- [47] Z. Moroz *et al.*, *AIP Conf. Proc.* **69**, 1102 (1981).
- [48] L. C. Chamon *et al.*, *Phys. Rev. C* **66**, 014610 (2002).
- [49] K. O. Pfeiffer, E. Speth, and K. Bethge, *Nucl. Phys.* **A206**, 545 (1973).

- [50] M. Biswas, Phys. Rev. C **77**, 017602 (2008); Nucl. Phys. **A802**, 67 (2008).
- [51] M. A. G. Alvarez *et al.*, Nucl. Phys. **A723**, 93 (2003).
- [52] L. C. Vaz, J. M. Alexander, and G. R. Satchler, Phys. Rep. **69**, 373 (1981).
- [53] R. K. Puri and R. K. Gupta, in *Proceedings of the International Conference on Heavy Ion Fusion: Exploring the Variety of Nuclear Properties, Padova, 1994*, edited by A. M. Stefanini, G. Nebbia, S. Lunardi, G. Montagnoli, and A. Vitturi (World Scientific, Singapore, 1994), p. 319.
- [54] P. R. S. Gomes *et al.*, Phys. Rev. C **71**, 034608 (2005).
- [55] C. Beck, N. Keeley, and A. Diaz-Torres, Phys. Rev. C **75**, 054605 (2007).
- [56] P. R. S. Gomes, J. Lubian, I. Padron, and R. M. Anjos, Phys. Rev. C **71**, 017601 (2005).
- [57] P. A. DeYoung *et al.*, Phys. Rev. C **71**, 051601(R) (2005).
- [58] H. Esbensen and G. F. Bertsch, Phys. Rev. C **66**, 044609 (2002).